solids

# Supplementary Materials: Structural and energetic aspects of entacapone-theophylline-water cocrystal.

Anna Karagianni, Julian Quodbach, Oliver Weingart, Anastasia Tsiaxerli, Vasiliki Katsanou, Vera Vasylyeva, Christoph Janiak and Kyriakos Kachrimanis

## 1. Methods

### 1.1. Construction of binary phase diagram

A molar ratio binary phase diagram was constructed by plotting the melting points against the molar ratio series of ENT-THP anhydrous physical mixtures. The mixtures were gently mixed in a mortar for 5 minutes. The melting points for the physical mixtures of different compositions ranging from 1:9 to 9:1 molar ratio, were determined by thermal analysis (DSC and HSM). DSC measurements were conducted to investigate the melting point assigned to ENT. As THP has a much higher melting point compared with that of ENT, it is difficult to detect the melting peak of THP in their physical mixtures by DSC, because degradation of ENT previously occurs. Therefore, HSM was applied to estimate the solubility of THP crystals and the melting point representing the temperature at which all crystals melted, as this could not be revealed via DSC. A binary phase diagram for ENT and THP monohydrate follows the same trend, after the early dehydration of THP.

### 1.2. Hansen Solubility parameters (HSP)

The Hansen solubility parameter (HSP) model is based on the partitioning of the total cohesive energy into the contributions of individual forces (dispersion, dipole–dipole/polar and hydrogen bonding) that hold the molecule intact [1]. The partial and total Hansen solubility parameter ($\delta_{t(Hansen)}$) were calculated using the atomic group contribution method of Hoftyzer-Van Krevelen [2], based on the following equations:

$$\delta_{t\,(Hansen)} = \sqrt{\delta_d^2 + \delta_p^2 + \delta_h^2} \quad (1)$$

$$\delta_d = \frac{\sum F_{di}}{V},\ \delta_p = \frac{\sqrt{\sum F_{pi}^{\,2}}}{V},\ \delta_h = \sqrt{\frac{\sum E_{hi}}{V}} \quad (2)$$

where $\delta_d$, $\delta_p$, and $\delta_h$ are the partial solubility parameters corresponding to the dispersive, polar, and hydrogen bonding forces, respectively. $F_{di}$ and $F_{pi}$ are the molar attraction constants due to dispersion and polar components, $E_{hi}$ is hydrogen bonding energy and $V$ is the molar volume.

The miscibility of the compounds was estimated using the solubility parameter difference ($\Delta\delta$), proposed by van Krevelen and Hoftyzer as following:

$$\Delta\delta = \sqrt{(\delta_{d2} - \delta_{d1})^2 + (\delta_{p2} - \delta_{p1})^2 + (\delta_{h2} - \delta_{h1})^2} \quad (3)$$

According to Mohammed et al., if the solubility parameter difference ($\Delta\delta$) between the API and the conformer is below 7 $MPa^{0.5}$, the components are considered as miscible and therefore likely to form a cocrystal [8].

The modified radius (*Ra*) between HSPs in Hansen three-dimensional space, where the partial solubility parameters are treated as coordinates, was calculated according to Eq (4):

$$Ra = \sqrt{(4 * \Delta\delta_p)^2 + (\Delta\delta_p)^2 + (\Delta\delta_h)^2} \quad (4)$$

The use of the modified radius (*Ra*) method with cut-off value of 17.64 $MPa^{0.5}$ has been proposed for cocrystal screening to estimate the solubility difference between cocrystal components [3,4].

**1.3. Molecular Complementarity (MC)**

For MC analysis [5], three geometrical descriptors (S-axis, S/L axis, and M/L axis; corresponding to the lengths of the shortest (S), medium (M), and longest (L) axes of the rectangular box surrounding the van der Waals volume of each molecule) and two polarity descriptors (fraction of nitrogen and oxygen, and dipole moment) were calculated for ENT and THP anhydrous pair and ENT and THP monohydrate pair, respectively. Ten different conformations of the submitted ENT crystal structure (CSD reference code OFAZUQ) were obtained using the CSD Conformer generator tool and evaluated against the coformers (THP anhydrous and THP monohydrate), whose starting coordinates were obtained from all CSD submitted cif files (CSD refcode for anhydrous THP: BAPLOT01, and for THP monohydrate: THEOPH, THEOPH01, THEOPH02, THEOPH03 and THEOPH04). The % hit rate and the "PASS" or "FAIL" flag was assessed. Incompatibility in at least one of the considered molecular descriptors results to a "FAIL" flag, while a "PASS" flag predicts a successful cocrystallization if and only if, all five descriptors exhibit a "PASS".

**1.4. Hydrogen Bond Propensity (HBP)**

HBP screening tool calculates the HBP values by estimating the probability of the formation of a specific hydrogen bond between defined functional groups, based on a training set of > 300 crystal structures [6]. This probability, i.e., propensity of this specific interaction between a donor-acceptor pair, is evaluated from its occurrence in a fitting dataset of CSD published crystal structures, using a logistic regression model. The HBP value for a specific hydrogen bond between the functional groups of the molecules are calculated between (a) API−coformer (heteromeric interactions) and (b) API−API and coformer−coformer (homomeric interactions). The calculation of the HBP were conducted for one only conformation of the molecules for the following CSD submitted crystal structures (CSD refcode a) ENT: OFAZUQ b) THP: BAPLOT01 c) THP monohydrate: THEOPH01). The multicomponent score was then calculated as the difference between highest HBP values ($\Delta_{HBP}$) for heterodimeric and homodimeric interaction for ENT-THP anhydrous and ENT-THP monohydrate pair. In case of $\Delta_{HBP} \geq 0$, cocrystallization is favoured.

## 2. Figures

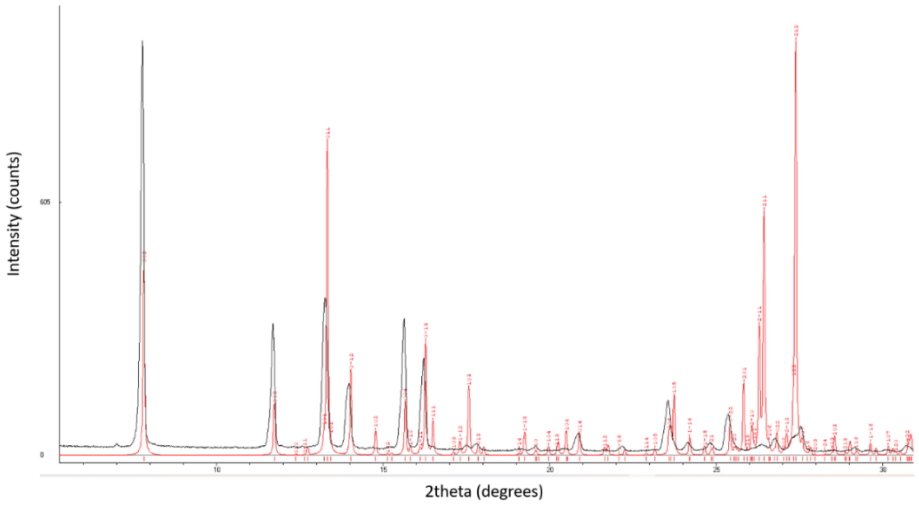


**Figure S1.** Experimentally obtained X-ray diffractogram of the cocrystal (black), superimposed on the theoretically calculated one (red) of the crystal structure retrieved from the CSD (CSD reference code XIPNOC).

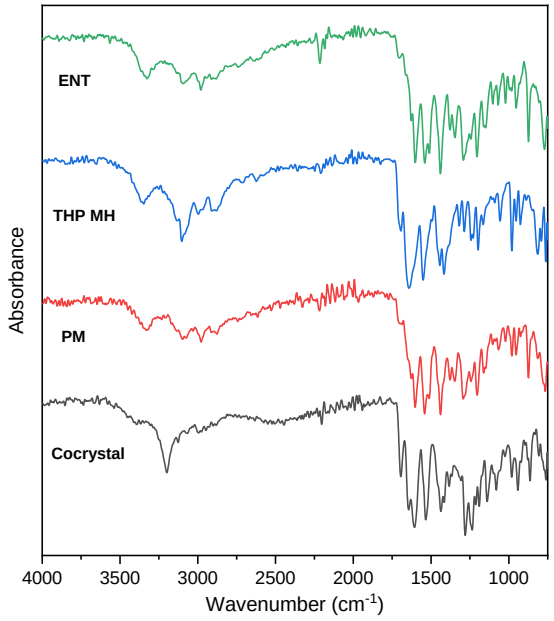


**Figure S2.** ATR-FTIR spectra of ENT, THP monohydrate (THP MH), their physical mixture (PM) and the ENT-THP-water 1:1:1 cocrystal.

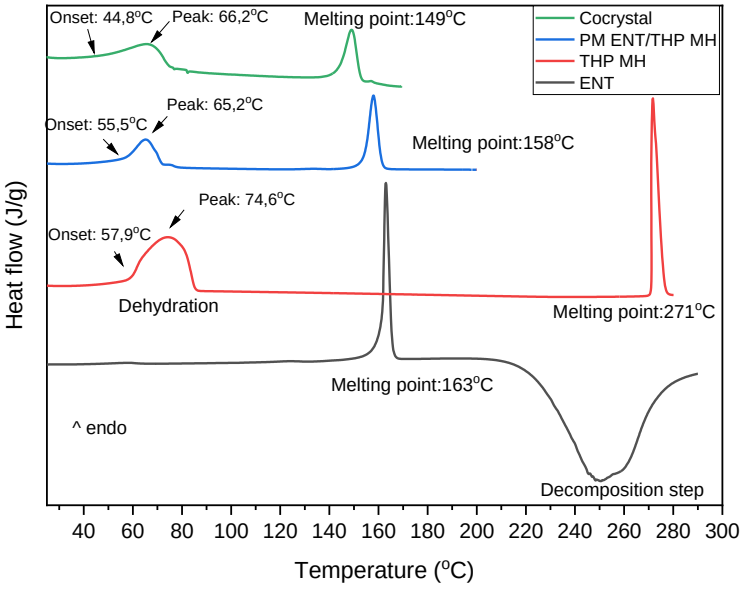


**Figure S3.** DSC thermographs for neat components, physical mixture and cocrystal.

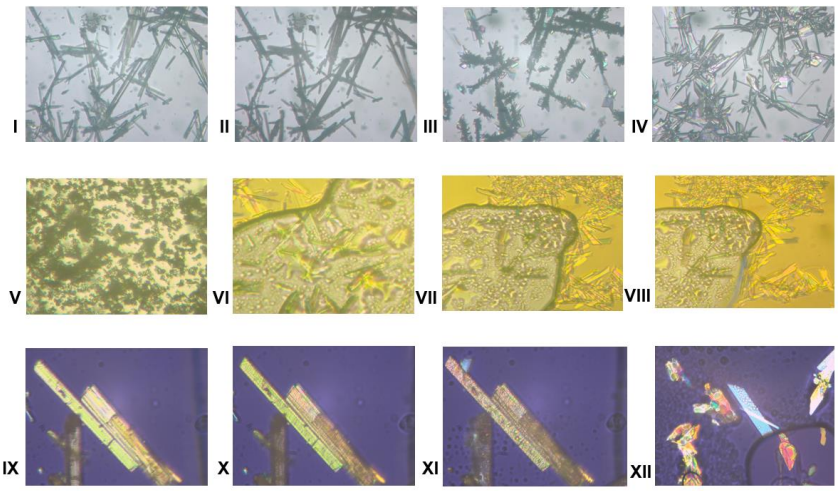


**Figure S4.** HSM micrographs of THP monohydrate, PM of ENT-THP monohydrate and ENT-THP-water 1:1:1 cocrystal.

Theophylline monohydrate: I) 25 °C, II) 70 °C (gradual loss of water), III) 215 °C (crystalline transformation after complete dehydration), IV) 270 °C (transition to THP anhydrous), Physical Mixture ENT-THP monohydrate 1:1: V) 25 °C, VI) 165 °C (melting of ENT), VII) 25 °C at second heating (THP crystals remained immiscible with the molten phase of ENT), VIII) 170 °C at second heating (immiscible THP crystals in the molten phase), ENT-THP-water 1:1:1 cocrystal: IX) 25 °C, X) 80 °C (rapid dissociation of the cocrystal after dehydration), XI) 150 °C (recrystallization of THP), XII) 200 °C (independent melting of the components).

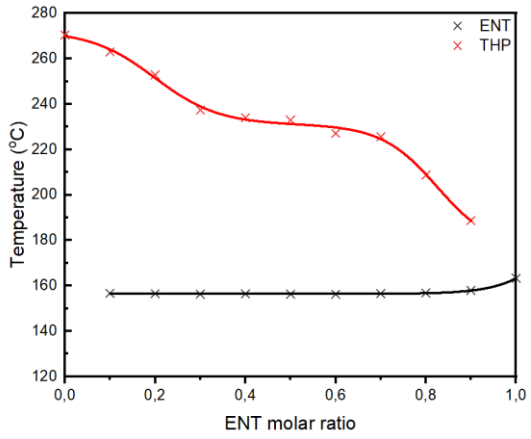


**Figure S5.** Binary phase diagram for different series of ENT:THP anhydrous 1:1 physical mixtures, showing two distinct melting points.

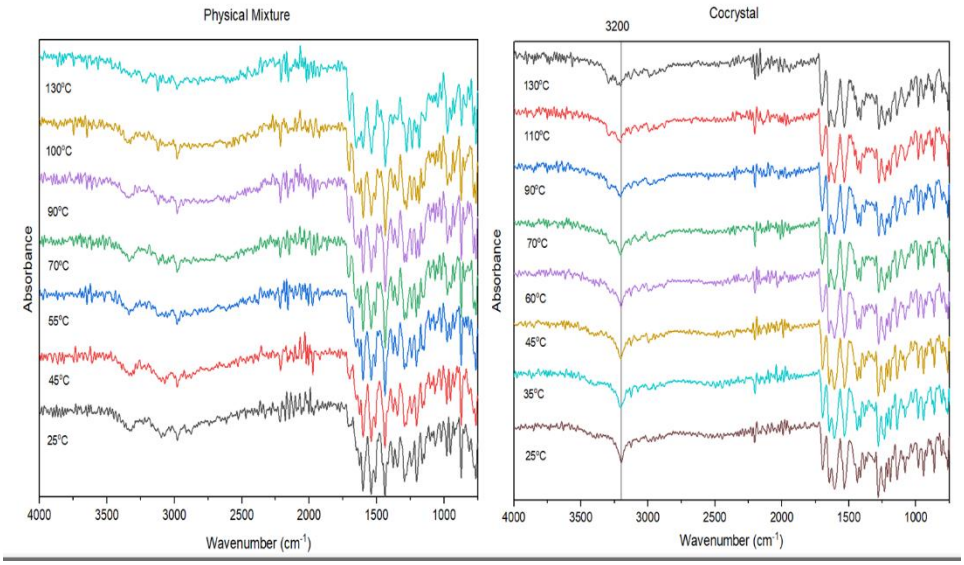


**Figure S6.** Variable temperature ATR-FTIR spectra for the 1:1 physical mixture of ENT:THP monohydrate and the ENT-THP-water 1:1:1 cocrystal.

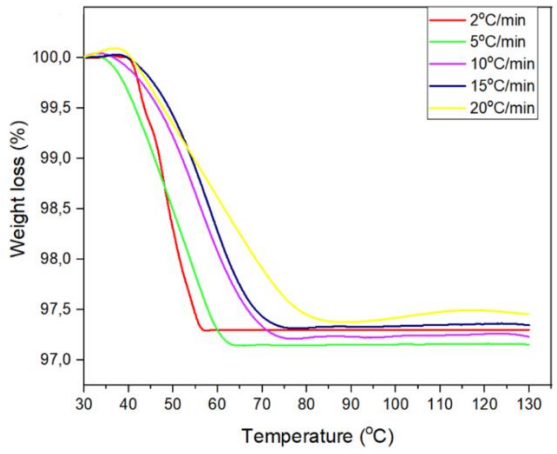


**Figure S7.** TGA curves of ENT-THP-water 1:1:1 cocrystal for 5 different heating rates.

## 3. Tables

**Table S1.** The total ($\delta_t$) and partial solubility parameters $\delta_d$, $\delta_p$, $\delta_h$ values of ENT and THP and the $\Delta\delta$ and *Ra* value calculated by Hoftyzer–Van Krevelen group contribution method (in $MPa^{1/2}$).

| | $\delta_d$ | $\delta_p$ | $\delta_h$ | $\delta_t$ |
|---|---|---|---|---|
| **Entacapone** | 24.12 | 11.29 | 16.39 | 31.27 |
| **Theophylline** | 17.88 | 8.5 | 12.58 | 23.46 |
| ***Δδ*** | | 7.83 | | |
| ***Ra*** | | 25.4 | | |

**Table S2.** Multicomponent score and highest propensity values for ENT (A) and coformers (B), obtained by HBP analysis.

| **Coformer (B)** | Multicomponent score | Highest Propensity Heterodimer | Homodimer |
|---|---|---|---|
| **Theophylline anhydrous** | -0.0 | 0.45 ±0.12 | 0.45 ±0.11 (B:B) |
| **Theophylline Monohydrate** | -0.02 | 0.62 ±0.10 | 0.65 ±0.09 (B:B) |

**Table S3.** Results of QM/MM geometry optimizations of crystal structure.

| **method** | **ENT-water (O-H···O) distance [Å]** | **Interaction energy (kcal/mol)** |
|---|---|---|
| PBE/6-31G** | 1.46 | 17.22 |
| PBE/6-31G**+BJ [1] | 1.43 | 18.63 |
| BHLYP/6-31G**+BJ [1] | 1.52 | 15.34 |
| M06L/6-31G**+D3 [2] | 1.53 | 14.43 |
| MP2/SV(P) | 1.50 | 16.86 |

[1] BJ: D3 with Becke-Johnson potential
[2] D3: Grimme Dispersion correction

**Table S4.** Correlation coefficient values of different mechanistic kinetics models for the dehydration process of ENT-THP-water 1:1:1 cocrystal (correlation coefficients with absolute values > 0.98 are highlighted in red).

| | **Correlation coefficient** | | | | |
|---|---|---|---|---|---|
| **Kinetic models** | **2 K/min** | **5 K/min** | **10 K/min** | **15 K/min** | **20 K/min** |
| D1 | -0.95702 | -0.95700 | -0.92986 | -0.96374 | -0.96688 |
| D2 (VC) | -0.96628 | -0.96641 | -0.94232 | -0.96850 | -0.97088 |
| D3 (Jander) | -0.97522 | -0.97524 | -0.95957 | -0.97074 | -0.97401 |
| D4 (GB) | -0.96971 | -0.96980 | -0.94828 | -0.96996 | -0.97217 |
| D5 (ZT) | -0.98483 | -0.98423 | -0.76138 | -0.72359 | -0.97531 |
| D6 (KU) | -0.95104 | -0.95057 | -0.91794 | -0.96036 | -0.96392 |
| n=3/2 | -0.98114 | -0.98093 | -0.95525 | -0.94054 | -0.97581 |
| n=1 | -0.98064 | -0.98009 | -0.95323 | -0.93824 | -0.97456 |
| n=2 | -0.97957 | -0.97825 | -0.94877 | -0.93323 | -0.97176 |

| | | | | | |
|---|---|---|---|---|---|
| n=3 | -0.97842 | -0.97615 | -0.94366 | -0.92761 | -0.96848 |
| n=4 | -0.97718 | -0.97373 | -0.93778 | -0.92129 | -0.96460 |
| | | | | | |
| R1 | -0.95405 | -0.95359 | -0.91793 | -0.96189 | -0.96339 |
| R2 | -0.96773 | -0.96906 | -0.93672 | -0.97014 | -0.97058 |
| R3 | -0.97165 | -0.97325 | -0.93667 | -0.96865 | -0.97271 |
| | | | | | |
| F1 | -0.98064 | -0.98009 | -0.95323 | -0.93830 | -0.97408 |
| F2 | -0.98635 | -0.98438 | -0.57254 | -0.47895 | -0.97081 |
| F3 | -0.98128 | -0.97710 | -0.50760 | -0.38640 | -0.96147 |
| | | | | | |
| P2 | -0.95196 | -0.94842 | -0.91233 | -0.95642 | -0.95874 |
| P3 | -0.94809 | -0.94126 | -0.89705 | -0.95029 | -0.95159 |
| P4 | -0.94375 | -0.93258 | -0.87782 | -0.94281 | -0.94248 |
| P5 | -0.93887 | -0.92195 | -0.85327 | -0.93360 | -0.93067 |
| P3/2 | -0.95650 | -0.95616 | -0.92817 | -0.96302 | -0.96610 |

## 4. Analysis of Supramolecular π-Stacking Interactions

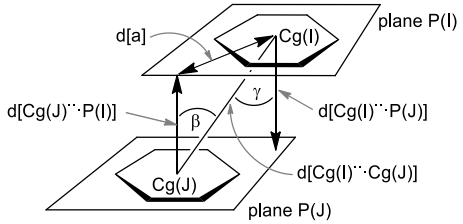


**Scheme S1.** Graphical presentation of the parameters used for the description of π-π stacking with the aid of PLATON [7].

The PLATON-listing of "Analysis of Short Ring-Interactions" for possible π-stacking interactions yielded significant π-π stacking with rather short centroid-centroid contacts (<3.8 Å), near parallel ring planes (alpha < 10° to ~0° or even exactly 0° by symmetry), small slip angles (β, γ <25°) and vertical displacements (slippage <1.5 Å) which translate into a sizable overlap of the aryl-plane areas [8].

**Table S5.** Packing analysis for possible π-π interactions for ENT and THP in ENT-THP-water 1:1:1 cocrystal. (see Scheme S1 for explanation).

==========

Analysis of Short Ring-Interactions with Cg-Cg Distances < 6.0 Ang., Alpha < 20.000 Deg. and Beta < 60.0 Deg.

==========

- Cg(I) = Plane number I (= ring number in () above)
- Alpha = Dihedral Angle between Planes I and J (Deg)
- Beta = Angle Cg(I)-->Cg(J) or Cg(I)-->Me vector and normal to plane I (Deg)
- Gamma = Angle Cg(I)-->Cg(J) vector and normal to plane J (Deg)
- Cg-Cg = Distance between ring Centroids (Ang.)
- CgI Perp = Perpendicular distance of Cg(I) on ring J (Ang.)
- CgJ_Perp = Perpendicular distance of Cg(J) on ring I (Ang.)
- Slippage = Distance between Cg(I) and Perpendicular Projection of Cg(J) on Ring I (Ang).
- P,Q,R,S = J-Plane Parameters for Carth. Coord. (Xo, Yo, Zo)

(only the symmetry-unique interactions are listed)

| Cg(I) | Res(I) | Cg(J) | [ARU(J)] | Cg-Cg | Alpha | Beta | Gamma | CgI_Perp | CgJ_Perp | Slippage |
|---|---|---|---|---|---|---|---|---|---|---|
| Cg(1) | [1] -> | Cg(2) | [1565.02] | 3.613(2) | 3.0(2) | 19.2 | 20.1 | 3.3921(15) | -3.4113(17) | 1.190 |
| Cg(1) | [1] -> | Cg(2) | [1665.02] | 4.661(2) | 3.0(2) | 45.3 | 43.2 | -3.3962(15) | 3.2791(17) | 3.313 |
| Cg(1) | [1] -> | Cg(3) | [1565.02] | 3.556(2) | 3.37(17) | 21.2 | 17.8 | 3.3847(15) | -3.3156(15) | 1.285 |
| Cg(1) | [1] -> | Cg(3) | [1665.02] | 3.588(2) | 3.37(17) | 19.9 | 17.0 | -3.4316(15) | 3.3747(15) | 1.219 |

[1565] = X,1+Y,Z
[1665] = 1+X,1+Y,Z

Cg1 = centroid of ring C1-C2-C3-C4-C7-C8 (ENT)
Cg2 = centroid of ring N4-N7-C15-C16-C20 (THP-imidazole)
Cg3 = centroid of ring N5-N6-C15-C16-C17-C18 (THP-pyrimidine)

**Table S6.** Packing analysis for possible Y-X…π interactions for ENT and THP in ENT-THP-water 1:1:1 cocrystal. (see Scheme S1 for explanation).

Analysis of Y-X...Cg(Pi-Ring) Interactions (X..Cg < 4.0 Ang. - Gamma < 30.0 Deg)

| Y--X(I) | Res(I) | Cg(J) | [ARU(J)] | X..Cg | X-Perp | Gamma | Y-X..Cg | Y..Cg | Y-X,Pi |
|---|---|---|---|---|---|---|---|---|---|
| N(1)- O(4) | [1] -> | Cg(2) | [1665.02] | 3.408(4) | -3.363 | 9.32 | 88.7(2) | 3.589(4) | 1.13 |
| C(18)- O(7) | [2] -> | Cg(1) | [1445.01] | 3.947(3) | 3.513 | 27.13 | 63.0(2) | 3.564(4) | 2.81 |

[1665] = 1+X,1+Y,Z
[1445] = -1+X,-1+Y,Z

Cg1 = centroid of ring C1-C2-C3-C4-C7-C8 (ENT)
Cg2 = centroid of ring N4-N7-C15-C16-C20 (THP-imidazole)

**References**

1. Hansen, C.M. The three-dimensional solubility parameter - key to paint component affinities: solvents, plasticizers, polymers, and resins. II. Dyes, emulsifiers, mutual solubility and compatibility, and pigments. III. Independent calculation of the parameter components. *J. Paint Technol.* **1967**, *39*, 505–510.

2. Breitkreutz, J. Prediction of Intestinal Drug Absorption Properties by Three-Dimensional Solubility Parameters. *Pharm. Res. 1998 159* **1998**, *15*, 1370–1375, doi:10.1023/A:1011941319327.
3. Vebber, G.C.; Pranke, P.; Pereira, C.N. Calculating hansen solubility parameters of polymers with genetic algorithms. *J. Appl. Polym. Sci.* **2014**, *131*, doi:10.1002/APP.39696.
4. Hansen, C.M. Methods of characterization - surfaces. *Hansen Solubility Parameters A Users Handbook, Second Ed.* **2007**, 113–123, doi:10.1201/9781420006834/HANSEN-SOLUBILITY-PARAMETERS-CHARLES-HANSEN.
5. Fábián, L. Cambridge structural database analysis of molecular complementarity in cocrystals. *Cryst. Growth Des.* **2009**, *9*, 1436–1443, doi:10.1021/cg800861m.
6. Galek, P.T.A.; Pidcock, E.; Wood, P.A.; Bruno, I.J.; Groom, C.R. One in half a million: a solid form informatics study of a pharmaceutical crystal structure. *CrystEngComm* **2012**, *14*, 2391–2403, doi:10.1039/C2CE06362J.
7. Spek, A.L. Structure validation in chemical crystallography. *Acta Crystallogr. Sect. D Biol. Crystallogr.* **2009**, *65*, 148–155, doi:10.1107/S090744490804362X.
8. Janiak, C. A critical account on π–π stacking in metal complexes with aromatic nitrogen-containing ligands. *J. Chem. Soc. Dalt. Trans.* **2000**, 3885–3896, doi:10.1039/B003010O.